THE JOURNAL OF PHYSICAL CHEMISTRY B

Article

pubs.acs.org/JPCB

On the Photophysics of Carotenoids: A Multireference DFT Study of Peridinin

Stefan Knecht,*[,†,‡] Christel M. Marian,[§] Jacob Kongsted,[‡] and Benedetta Mennucci[∥]

[†]Laboratory of Physical Chemistry, ETH Zürich, Wolfgang-Pauli-Straße 10, 8093 Zürich, Switzerland

[‡]Department of Physics, Chemistry and Pharmacy, University of Southern Denmark, Campusvej 55, 5230 Odense M, Denmark

[§]Institute of Theoretical and Computational Chemistry, University of Düsseldorf, Universitätsstraße 1, 40225 Düsseldorf, Germany

[∥]Dipartimento di Chimica e Chimica Industriale, Università di Pisa, via Risorgimento 35, I-56126 Pisa, Italy

Supporting Information

ABSTRACT: We present a quantum-mechanical investigation of the photophysics of a specific carotenoid, peridinin, which is present in light-harvesting complexes. The fundamental role played by the geometry in determining the position and character of its low-lying singlet electronic states is investigated using a multireference DFT approach in combination with a continuum solvation model. The main photophysical properties of peridinin appear to be governed by the lowest two singlet excited states, as no evidence points to an intermediate S* state and the energies of the upper excited states are too high to allow their population with excitation in the visible range. These two excited states (S_1, $2^1A_g^-$ and S_2, $1^1B_u^+$) are highly connected through the conjugation path here characterized by the value of the bond length alternation (BLA). The S_1 and S_2 states present distinct natures for small BLA values, whereas for larger ones they become more similar in terms of both brightness and dipolar character and their energies become closer. The geometrical issue is thus of fundamental importance for a correct interpretation of the spectroscopic signatures of peridinin.

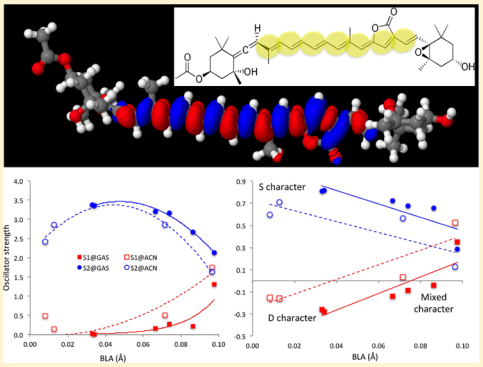

1. INTRODUCTION

Carotenoids are naturally occurring pigments that absorb light in the spectral region in which the sun irradiates maximally (450−550 nm); owing to this characteristic, they are often present in natural light-harvesting (LH) pigment−protein complexes where they act as donors of electronic energy to (bacterio)chlorophylls [(B)Chls].[1] In addition, carotenoids play a photoprotective role for the same complexes by quenching all the dangerous products (chlorophyll triplet and oxygen singlet states) generated by an excess of light.[2−4] Over 1000 naturally occurring carotenoids are known. In all cases, the common structural feature is a linear chain of alternating C—C single and C═C double bonds, while they differ in π-electron conjugation length (number of conjugated double bonds, N) and in the type and number of functional groups attached to the carbon backbone.

Due to this structural feature, the photophysics of the carotenoids has generally been interpreted in terms of two low-lying excited singlet states, called S_2 ($1^1B_u^+$) and S_1 ($2^1A_g^-$).[5] According to optical selection rules, the one-photon-allowed transition from the ground state S_0 ($1^1A_g^-$) goes to S_2, which then internally converts to S_1 in a few hundred femtoseconds. Singlet−singlet excitation energy transfer from carotenoids to chlorophylls has been described, depending on the antenna complex involved, as going either from S_2 to the chlorophyll Qx excited state or from S_1 to the Qy state; in some complexes, both pathways are active.[1] The energy transfer efficiency of each of the possible pathways depends on the conjugation length N of the carotenoid and on the functional groups attached to the carbon backbone. Whereas the S_2-mediated energy transfer is nearly constant (ca. 50%) for carotenoids with N = 9−11 and decreases to 30% for N > 12, the S_1 route reaches 90% efficiency for N = 9 and drops to less than 10% for N > 11. This strong dependence is ascribed to the change in the spectral overlap between the carotenoid S_1 state and Qy band of (B)Chl's. For some carotenoids, this two-state model has been further generalized to include additional state(s) lying between the S_1 and S_2 states.[6−12] In particular, some experiments have suggested the existence of a third, potentially relevant excited state (that is not the $1^1B_u^-$ state), generally indicated as the S* state; however, its real existence and nature is currently still under debate.[13] Very recently, a hypothesis has been proposed to explain the experimental evidence by assuming two thermally populated ground state isomers with the higher one generating the S* state, which can be effectively frozen out by cooling.[14]

In some types of LH complexes such as the peridinin−chlorophyll protein (PCP) from dinoflagellates, carotenoids

Received: August 6, 2013
Revised: October 2, 2013
Published: October 3, 2013

   dx.doi.org/10.1021/jp4078739 | J. Phys. Chem. B 2013, 117, 13808−13815

contain a conjugated carbonyl group (see the structure reported in the upper part of Figure 1). Due to this moiety,

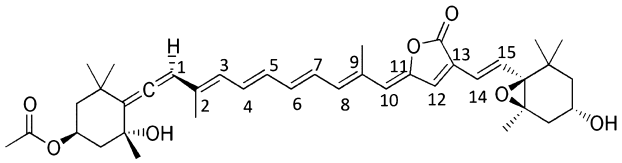

BLA	State	GAS	ACN
@crystal	S_0	0.086	
@CAM	S_0	0.098	0.096
@B3LYP	S_0	0.074	0.072
@MP2	S_0	0.067	-
@TDCAM	S_2	0.034	0.008
@TDB3LYP	S_2	0.033	0.013

Figure 1. Bond length alternation (BLA) (in Å) calculated at different QM levels for both the ground (S_0) and S_2 excited states in the gas phase (GAS) and in acetonitrile (ACN) solution. Atomic centers included in the definition of BLA are indicated with numbers from 1 to 15. CAM is an abbreviation for CAMB3LYP.

the resulting peridinin carotenoid shows spectroscopic features and excited state dynamics which are more dependent on the polarity of the environment than those of other carotenoids.[15] To explain such a specific behavior of peridinin, the presence of an intramolecular charge-transfer (ICT) excited state has been proposed.[16,17] It is thought that the energy of the ICT state can be either stabilized or destabilized relative to the S_1 state depending on the polarity of the environment, thereby affecting the excited-state spectra and dynamics of the molecule. Due to a strong S_1−ICT coupling, these two states have never been separated, and they have been described as a collective S_1/ICT state which can transfer energy to chlorophyll in competition with the S_2 channel.[18] As a matter of fact, it remains uncertain whether the ICT state is a separate electronic state from S_1,[19,20] is mixed with it,[21] or simply is the S_1 state with a large intrinsic dipole moment stemming from a mixing with the S_2 state.[22]

The photophysics of peridinin and similar carotenoids have also been studied by theoretical methods.[5,15,22−33] Because of the large dimension of the system, most of the first theoretical information was derived by semiempirical calculations[5,22,23,32] or by *ab initio* methods applied to model systems.[30] The quantum mechanical (QM) simulation of the S_1 state was, and still is, a challenging task due to its strong multiconfigurational character. A wave function analysis reveals that S_1 is comprised of as leading configuration a double excitation from the highest occupied molecular orbital (HOMO) to the lowest unoccupied molecular orbital LUMO—"(HOMO → LUMO)^2"—that mixes considerably with increasing π-electron conjugation length N with the "HOMO−1 → LUMO", "HOMO → LUMO+1", and "HOMO → LUMO" single excitations. This composition is a distinct feature of the S_1 state in all polyenes with $N > 1$;[5,27,34,35] indeed, standard single reference methods cannot localize it, while the S_2 state, that exhibits a significant charge-transfer character,[36] can be more easily calculated and in many QM methods this state appears as the lowest singlet excited state. Time-dependent density functional theory (TD-DFT) methods have also been used, but the results are strongly dependent on the selected functional even if generally the lowest excited state is found to be the experimental S_2 bright state. Only some specific combinations of functionals and basis sets gave a lowest state with a dark S_1-like character.[24,25,28] This peculiar finding has been carefully traced back to a fortuitous cancellation of errors[27] where, contrary to the wave function analysis (*vide supra*), TD-DFT represents the S_1 state as a combination of two single excitations "HOMO−1 → LUMO" and "HOMO → LUMO+1", respectively. However, DFT combined with a multireference configuration interaction *ansatz* as in the DFT/MRCI method[30,37] has been shown to be a quite accurate—with errors less than 0.2 eV for organic systems[29,38]—and reliable approach that not only yields the correct order of the lowest excited states in carotenoids[29−31,33] but also gives a reasonable ground- and excited-state wave function picture.

The present work addresses the characterization of the low-energy part of the spectrum of peridinin and the nature of the related excited states using a DFT/MRCI description of the electronic states in combination with different geometries, either measured or calculated, and solvent effects. This strategy allows us to elaborate on the relevance of the geometrical effects on the relative position and the intrinsic nature of the two lowest excited states and how these effects can combine with a polarizable environment.

2. COMPUTATIONAL DETAILS

All (TD)DFT geometry optimizations were performed in the Gaussian code[39] using the 6-31G(d) basis set for both gas-phase and solvated systems, since analytical gradients for the DFT/MRCI approach are not available yet. Due to its computational cost, an MP2 geometry optimization was done in Turbomole[40] using the cc-pVDZ basis set only for the gas-phase system. The excited state TD-DFT structures were optimized for the excited state which corresponds to the bright S_2 state: a reliable description of the dark S_1 state was in fact not feasible at the TD-DFT level. Solvent effects were introduced using the polarizable continuum model (PCM)[41] in its integral equation formalism (IEF-PCM)[42] version.

All DFT/MRCI calculations were carried out following the computational recipe that was previously successfully applied to study β-carotene isomers.[31] We used a split valence basis set (def-SV(P))[43] for all atoms that is augmented with a d-polarization function on all non-hydrogen atoms. The configuration state functions in the MRCI expansion for the gas phase, and solution calculations were built from KS orbitals using the BH-LYP[44,45] functional as implemented in the Turbomole 6.3[40] program package. Keeping the 1s electrons of the heavy atoms frozen in the post-SCF step, the initial MRCI reference space was spanned by all single and double excitations from the five highest occupied MOs to the five lowest unoccupied MOs of the ground state KS determinant.[46] Using an orbital selection threshold of 0.6 E_h, the lowest 12 eigenvectors were computed. The resulting reference space for the subsequent DFT/MRCI run was then chosen to comprise all configurations contributing to one of the 12 lowest-lying eigenvectors of the initial DFT/MRCI calculation with a squared coefficient of 0.003 and larger. In this second step, we optimized the ground and lowest seven electronically excited states of peridinin.

The IEF-PCM approach is not implemented at the SCF and DFT/MRCI level in Turbomole. Thus, rather than invoking at the SCF level the COSMO solvent model as implemented in Turbomole, we have chosen to represent the solvent in the SCF and DFT/MRCI calculations as point charges that were

dx.doi.org/10.1021/jp4078739 | J. Phys. Chem. B 2013, 117, 13808−13815

exported from the PCM calculations performed in the Gaussian code at the (TD)DFT level of calculation at the corresponding geometries. This procedure constitutes a reasonable approach to include the solvent effect in the DFT/MRCI calculations: in doing so, we can in fact introduce solvent effects into the multireference description of the system even if we neglect the back-effect, e.g., the effect of the electronic charge distribution of the system on the solvent polarization.

3. RESULTS AND DISCUSSION

3.1. The Geometrical Issue. In order to unequivocally characterize the main geometrical properties of peridinin, we made use of a structural parameter known as "bond length alternation" (BLA). Such a parameter, which is defined as the difference between the average length of the carbon−carbon single and double bonds, has been widely used in the literature focusing on the structure and properties of long conjugated molecules (especially push−pull systems)[47−49] for which electronic states can be represented in terms of two resonance limit forms showing a neutral and a zwitterionic character, respectively: by definition, a positive BLA value is associated with the neutral form, a negative value to the zwitterionic form, and a value of zero to a completely delocalized system. In the present case, the definition of the BLA parameter includes the polyene backbone of peridinin as labeled in the upper part of Figure 1, namely, all bonds between atoms 1−15. The lower part of Figure 1 then comprises the BLA values obtained by optimizing the geometry at different QM levels for both isolated and acetonitrile-solvated systems. In addition to BLA values corresponding to geometries optimized for the S_0 ground state, we also give values obtained for the relaxed bright S_2 state (obtained at TD-CAMB3LYP and TD-B3LYP levels) as well as the BLA data referring to the experimental crystal structure of PCP.[50]

As it can be seen from the BLA values, the effects of both exchange and correlation are not negligible, with MP2 giving the smallest ground-state BLA followed by B3LYP and successively CAMB3LYP. We recall that the larger (and more positive) the BLA is, the more localized is the conjugation path into separate single and double bonds as predicted by a simple Lewis picture. Both DFT functionals, when applied to the excited state S_2, significantly reduce the BLA, indicating a more delocalized distribution upon excitation to this bright state. Including the effects of the solvent affects the ground-state BLA only slightly, while it further reduces the BLA for the excited state. Indeed, this reduction is an indication of a larger solvent sensitivity related to the S_2 state in comparison with the S_0 ground state. In particular, it is worth noting that at the TD-CAMB3LYP level the BLA in acetonitrile almost goes to zero; i.e., the system can be represented as completely delocalized.

From now on, these different structures will be used to quantify and interpret the nature of both the ground and two lowest excited states and their eventual tuning due to changes in the conjugation path. The third excited state is not reported in the analysis, as it remains always well above the S_2 state (by about 0.3−0.6 eV) and with very low oscillator strengths independent of the BLA.

3.2. Ground- and Excited-State Properties. To begin the analysis, we first focus on the composition of the different states of interest. In Table 1, we provide the contributions (in percent) from the reference determinant (KS), the HOMO → LUMO, and (HOMO → LUMO)^2 configurations for the three states considered, i.e., S_0, S_1, and S_2. These contributions are tabulated for geometries obtained either from gas-phase (GAS) or acetonitrile (ACN) solution calculations. Note that, as previously explained, the DFT/MRCI calculations including acetonitrile solvent are based on PCM charges obtained at the DFT level (either B3LYP or CAMB3LYP according to the geometry used). In Table 1, we have only included the contributions from the HOMO → LUMO and (HOMO → LUMO)^2 configurations, although as previously noted also the HOMO−1 → LUMO and HOMO → LUMO+1 configurations may gain in significance. However, the trends related to these configurations are similar to the HOMO → LUMO configuration and for clarity we have chosen to put particular emphasis on this configuration.

Table 1. Percentage Contributions of the Reference Determinant (KS), the HOMO → LUMO, and (HOMO → LUMO)^2 Configurations to the Three States Considered (S_0, S_1, and S_2) for Different BLA Values[a]

GAS				ACN			
BLA	S_0	S_1	S_2	BLA	S_0	S_1	S_2
KS							
0.098	89	1	1	0.096	89	0	1
0.086	86	2	1	0.072	87	2	1
0.074	86	2	1	0.013	77	9	1
0.067	86	3	1	0.008	77	10	0
0.034	81	6	0				
0.033	81	6	0				
HOMO → LUMO							
0.098	0	46	39	0.096	0	60	25
0.086	0	14	69	0.072	0	22	62
0.074	0	14	71	0.013	1	3	74
0.067	0	11	73	0.008	1	14	62
0.034	0	2	82				
0.033	0	2	81				
(HOMO → LUMO)^2							
0.098	1	12	10	0.096	1	8	13
0.086	2	18	3	0.072	2	19	6
0.074	2	22	3	0.013	8	31	0
0.067	3	24	3	0.008	7	29	2
0.034	6	30	1				
0.033	5	28	1				

[a]The GAS results refer to calculations in the gas phase, and the ACN results refer to calculations performed in acetonitrile solution.

As clearly seen from Table 1, the weight of the reference (KS) configuration of the ground state presents a homogeneous behavior with BLA values, while the contribution from the double excitation behaves in an opposite way; i.e., the multiconfigurational nature increases for a decreasing BLA. This picture holds both in the gas phase and in acetonitrile solution.

It is furthermore evident from the results reported in Table 1 that the two excited states behave completely opposite with respect to their composition for varying BLA values. For S_1, the weight of the reference (KS) configuration increases, the weight of the single HOMO → LUMO excitation decreases notably, and the weight of the double excitation (HOMO → LUMO)^2 increases significantly as a function of decreasing BLA, while the opposite is true for the S_2 state. These findings are in line with the trends observed for the carotenoid lutein upon geometrical distortion,[51] which leads to a disruption of the conjugation path.

dx.doi.org/10.1021/jp4078739 | J. Phys. Chem. B 2013, 117, 13808−13815

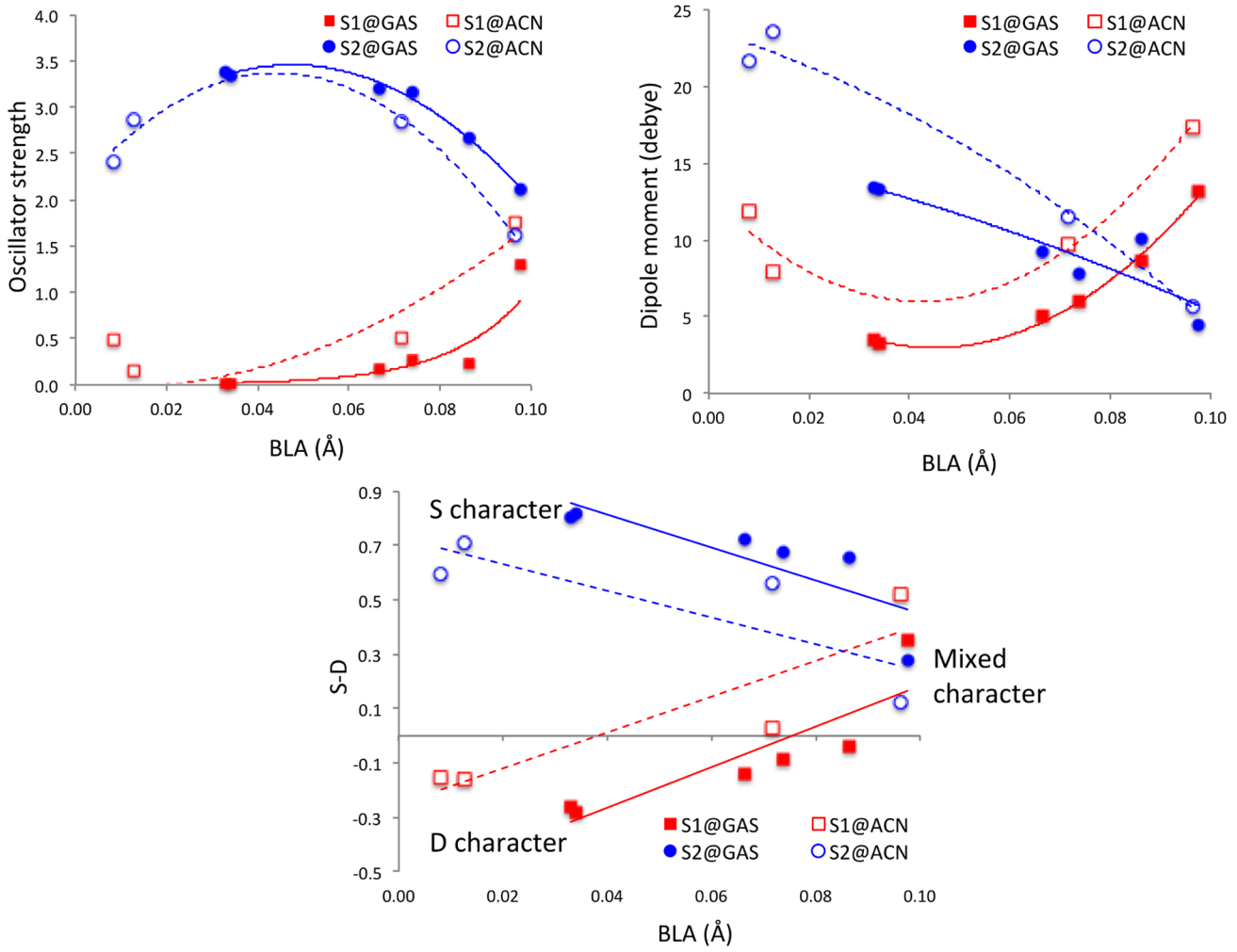

Figure 2. BLA dependence of oscillator strength (left upper), dipole moment (right upper), and differences in single (S) and double (D) excitation character of the S_1 and S_2 excited states calculated in the gas phase and in acetonitrile (ACN). The solid (gas phase) and dashed (in acetonitrile) lines connecting the calculated points are guides for the eye.

Due to the dependence of the wave function composition on the BLA, we expect that transition and state properties are accordingly tuned by BLA variations. Such a correlation is indeed encountered, as revealed from Figure 2 where we report the oscillator strengths of the two excitations as well as the dipole moment of each excited state as a function of the BLA. To further emphasize the direct correspondence between the wave function composition and the two selected properties in Figure 2, we also provide a graphical representation of the single and double character of the wave function of the two excited states when changing BLA. In all cases, results in both the gas phase and acetonitrile solution are shown.

The results in the upper panel (oscillator strengths and dipole moments) support the conclusion that as the BLA parameter increases the dark S_1 state becomes less dark while the bright S_2 state becomes less bright. Furthermore, from the change in the dipole moment, we can conclude a large solvent effect: in the polar solvent for BLAs larger than 0.075 Å, the two states invert the magnitude of their dipoles with S_1 showing a larger dipole moment than S_2 (in a vacuum, the trend is similar but the two dipoles never invert). The dipole moment of the S_0 ground state, in turn, is less sensitive to the BLA with values of ∼3.6−4.1 D in a vacuum and ∼5.5−8.8 D in acetonitrile. These findings can be correlated with a CT character of the states, due to a charge reorganization upon excitation from the allene tail along the conjugation path toward the lactone ring. As a matter of fact, from our calculations, we find that both states present a CT character with S_1 showing a larger charge reorganization (see Figure S1 in the Supporting Information).

Finally, if we combine the two graphs on oscillator strengths and dipoles with the third one summarizing the relative importance of single and double contributions, a clear picture emerges: the two excited states are "connected" through the conjugation path. When the structure allows for a more delocalized picture (small BLA values), the two states present a distinct nature with S_1 (S_2) showing a dominant double (single) character which also corresponds to a dark (bright) and an apolar (dipolar) nature. By increasing the localization (e.g., for larger BLA values), instead, the two states become more and more similar both in terms of brightness and dipolar character: this increased similarity is clearly marked by the convergence of the S−D values for large BLAs. To make the connection between the wave function composition and the properties associated with the specific states even more evident, we have plotted in Figure 3 the dependence on the dipole moment and the oscillator strength with respect to the difference between single and double character.

dx.doi.org/10.1021/jp4078739 | J. Phys. Chem. B 2013, 117, 13808−13815

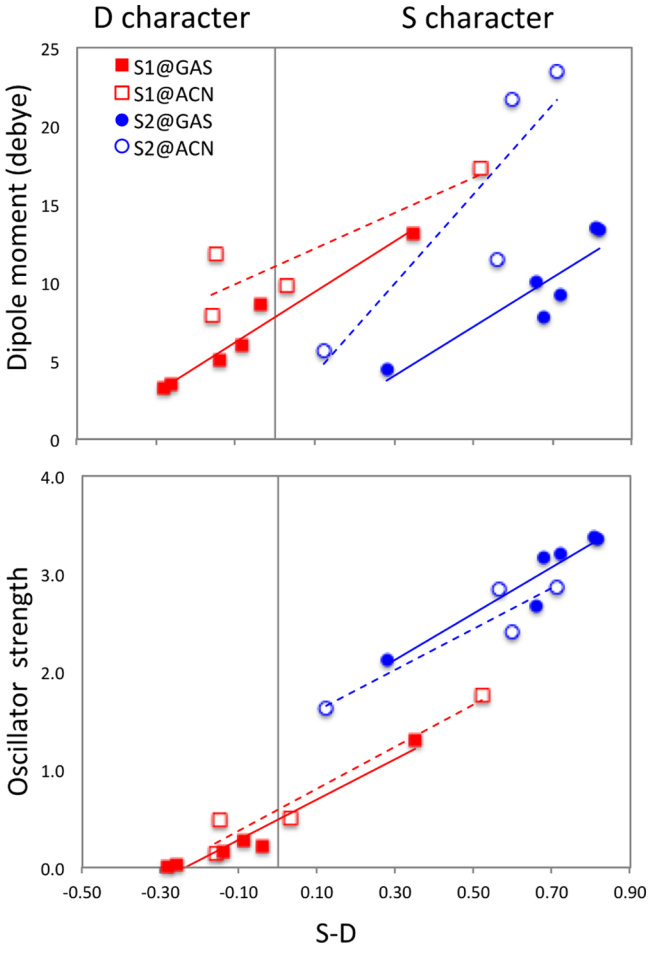

Figure 3. Dependence of the dipole moment (upper panel) and oscillator strength (lower panel) on differences in single (S) and double (D) excitation character for S_1 and S_2 excited states calculated in the gas phase and in acetonitrile (ACN). The solid (gas phase) and dashed (in acetonitrile) lines connecting the calculated points are guides for the eye.

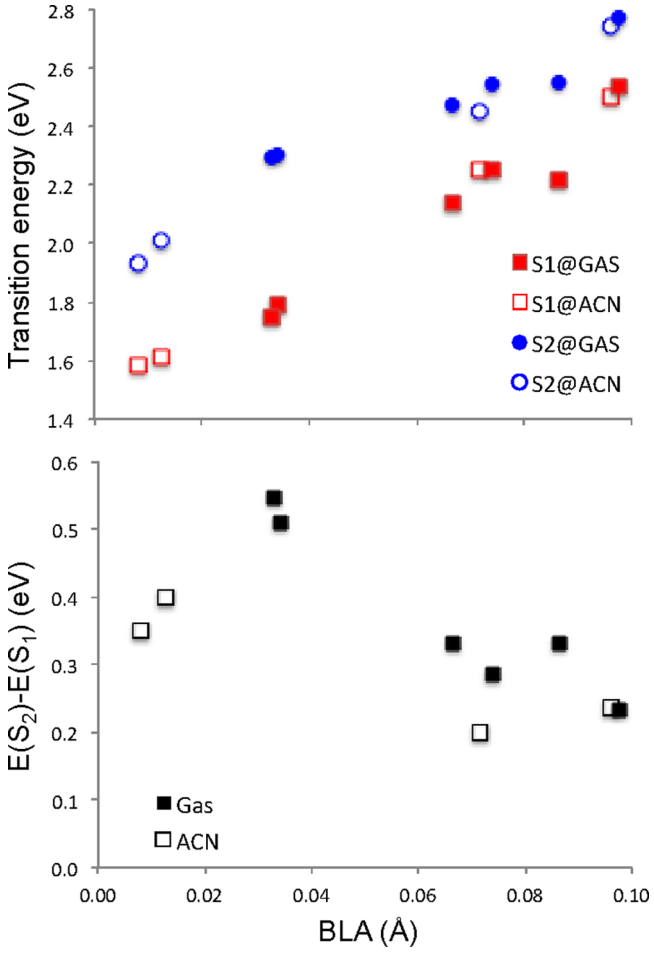

Figure 4. Vertical absorption energies (in eV) vs BLA (upper panel) and differences between the first two excited states (S_2–S_1) (lower panel) calculated in gas and in acetonitrile (ACN) as a function of the BLA parameter.

From this figure, the suggested correlation between bright character and dipole moment (*vide supra*) is quantified: states with a dominating "HOMO → LUMO" singles contribution are bright and possess a large dipole moment, whereas states which are dominated by a double excitation and/or "HOMO → LUMO+1" and "HOMO−1 → LUMO" single excitations, respectively, are dark and possess a small dipole moment.

The observed dependence of the ground and excited state wave functions on the BLA is finally reflected in the relative transition energies, as shown in Figure 4.

As can be seen from the upper graph of Figure 4, there is a clear correlation between the transition energies and the BLA for both S_0–S_1 and S_0–S_2 excitations. Indeed, by increasing the BLA, also the excitation energies increase for both the isolated and solvated systems. This trend is in qualitative agreement with the expected picture emerging from a simple particle-in-a-box picture: by decreasing the BLA closer to zero, the system becomes close to a perfect conjugation, which, due to the inverse dependence on the excitation energies and the length of the conjugated chain, means that the excitation energies should decrease. We note, however, that the increase/decrease in excitation energies is not equal for the two excitations and as a result the two excited states become closer in energy as the BLA increases (see lower panel).

These findings clearly indicate that, in order to make a correct prediction of the photophysical behavior of peridinin, it is of utmost importance that the underlying electronic structure method used is accurate. This prerequisite is due to the fact that even small deviations in the BLA lead to significant changes in the properties of these two states and thereby also in their interpretation. As such, a proper account of the solvent (or more generally the environment) is also very important, since the environment may induce non-negligible changes to the BLA as well as it can differently affect the excited states that govern the photophysics of peridinin.

3.3. Comparison to Experiments. Finally, we provide a comparison of our results with experimental data obtained in solution.[52] For this analysis, we have selected the (TD-)B3LYP geometries, as this functional has shown to be more consistent (for the S_0 state) as compared to the correlated MP2 one (regarding the excited state structures, the choice of the functional appears less delicate, as shown by the almost equivalent values of the BLAs obtained with TD-B3LYP and TD-CAMB3LYP). In the simulation of the fluorescence spectrum, we have assumed that the geometry relaxation in the S_2 state is faster than the internal conversion to the S_1 state and that the emission comes from an unrelaxed S_1 state. The

dx.doi.org/10.1021/jp4078739 | J. Phys. Chem. B 2013, 117, 13808–13815

assumption that the primary emission of peridinin occurs from S_1 is largely accepted due to the fact that its fluorescence spectrum is significantly Stokes-shifted. Table 2 compiles a comparison between computational and experimental data for both absorption and emission energies. For completeness, absorption and emission energies for the S_3−S_7 states are given in Table S1 in the Supporting Information.

Table 2. Calculated and Experimental Absorption and Emission Energies in the Gas Phase (GAS) and in Acetonitrile (ACN)[a]

	calc	exp	error
	absorption		
GAS	2.54	2.73[b]	−0.19
ACN	2.45	2.63	−0.18
	fluoresence		
GAS	1.75	1.74[b]	0.01
ACN	1.61	1.58	0.03
	Stokes shift		
GAS	−0.79	−0.99[b]	0.20
ACN	−0.84	−1.04	0.20

[a]Stokes shifts are also reported. All calculated values refer to (TD)B3LYP optimized geometries, and transition energies are given in eV. [b]Measured in *n*-hexane.

The agreement obtained is quite good for both photophysical processes with errors below 0.2 eV which is what could be expected for DFT/MRCI.[29,38] The nearly perfect coincidence between calculated and experimental fluorescences is surely fortuitous but also indicates that our assumption on the geometry of the emitting state is reasonable. In addition, the semiquantitative reproduction of the Stoke shift and its solvent dependence makes us confident that our computational strategy contains all the main ingredients required to get a realistic picture of the photophysics of peridinin, namely, (i) a multireference QM description, (ii) a proper consideration of the variation in the BLA upon excitation, and (iii) inclusion of electrostatic effects for solvation. These ingredients have here been effectively applied to peridinin in the gas phase and in an homogeneous solution; when a more complex environment such as a protein matrix is considered, it is possible that further specificities have to be added. However, the analysis reported here can still be used to extrapolate some more general conclusions also for peridinin-containing light-harvesting complexes.

4. CONCLUSIONS

In this contribution, we investigated the photophysics of the carotenoid peridinin revealing an intrinsic interplay between structure—particularly characterized by the bond length alternation (BLA) parameter—and solvent as well as position and character of the low-lying singlet electronic states. The main photophysical properties of peridinin appear to be governed by the lowest two singlet excited states, S_1 ($2^1A_g^-$) and S_2 ($1^1B_u^+$), respectively, as no evidence points to an intermediate S* state and the energies of the upper excited states are too high to allow their population with excitation in the visible range.

In particular, it is clear that the geometrical issue, expressed in the magnitude of the BLA parameter, is fundamental in order to interpret the spectroscopic signatures of peridinin: our results indicate that even small fluctuations in the BLA values can significantly modify the character of the excited states and their spectroscopic properties and largely affect the relative position of the corresponding transition energies. In addition, a similar dependence on the conjugation path is expected also for the vibrational excitations of carbon−carbon bonds which largely determine the vibrational progressions in the electronic spectra.

In summary, all of these outcomes make peridinin a very tunable system with respect to its capacity to act as an antenna. From our calculations, we could in principle predict that changes in the solvent polarity as well as in specific intermolecular interactions with solvent molecules and/or specific residues in a protein matrix significantly influence the photophysical properties of the system even through small changes in the structural characteristics. This flexibility could thus provide the possibility to adapt the preferable energy transfer pathway as a function of given external conditions.

Clearly, this investigation cannot be considered as conclusive to explain the complex photophysics of peridinin and its antenna function in light-harvesting complexes. However, we are confident that our findings will spur further investigations along the same lines and can be used as effective tools to achieve a more univocal interpretation of the experimental evidence.

■ ASSOCIATED CONTENT

Supporting Information

Figure S1 describes the variation of the Mulliken charge distribution in peridinin upon excitation. Table S1 summarizes the calculated absorption and emission energies in the gas phase and solution for the S_1−S_7 excited states computed at the DFT/MRCI level at the respective optimized (TD-)B3LYP geometries. Tables S2−S11 comprise all optimized structures referred to in this work. All structures given in Tables S2−S11 have been additionally listed in the same order in a single XYZ file. This material is available free of charge via the Internet at http://pubs.acs.org.

■ AUTHOR INFORMATION

Corresponding Author

*E-mail: stefan.knecht@phys.chem.ethz.ch.

Notes

The authors declare no competing financial interest.

■ ACKNOWLEDGMENTS

S.K. gratefully acknowledges a postdoctoral research grant from the Natural Science Foundation (FNU) of the Danish Agency for Science, Technology and Innovation (Grant No. 10-082944). J.K. thanks the Danish Center for Scientific Computing, The Danish Councils for Independent Research (STENO and Sapere Aude programmes), the Lundbeck Foundation, and the Villum foundation for financial support. B.M. acknowledges the European Research Council (ERC) for financial support in the framework of the Starting Grant (EnLight - 277755)

■ REFERENCES

(1) Polivka, T.; Frank, H. A. Molecular factors controlling photosynthetic light harvesting by carotenoids. *Acc. Chem. Res.* **2010**, *43*, 1125−1134.

(2) Holt, N. E. Carotenoid cation formation and the regulation of photosynthetic light harvesting. *Science* **2005**, *307*, 433−436.

(3) Kloz, M.; Pillai, S.; Kodis, G.; Gust, D.; Moore, T. A.; Moore, A. L.; Van Grondelle, R.; Kennis, J. T. M. Carotenoid photoprotection in artificial photosynthetic antennas. *J. Am. Chem. Soc.* **2011**, *133*, 7007−7015.
(4) Zaks, J.; Amarnath, K.; Kramer, D. M.; Niyogi, K. K.; Fleming, G. R. A kinetic model of rapidly reversible nonphotochemical quenching. *Proc. Natl. Acad. Sci. U.S.A.* **2012**, *109*, 15757−15762.
(5) Tavan, P.; Schulten, K. Electronic excitations in finite and infinite polyenes. *Phys. Rev. B* **1987**, *36*, 4337−4358.
(6) Cerullo, G.; Polli, D.; Lanzani, G.; De Silvestri, S.; Hashimoto, H.; Cogdell, R. J. Photosynthetic light harvesting by carotenoids: detection of an intermediate excited state. *Science* **2002**, *298*, 2395−2398.
(7) Rondonuwu, F. S.; Yokoyama, K.; Fujii, R.; Koyama, Y.; Codgell, R. J.; Watanabe, Y. The role of the $1^1B_u^-$ state in carotenoid-to bacteriochlorophyll singlet-energy transfer in the LH2 antenna complexes from Rhodobacter sphaeroides G1C, Rhodobacter sphaeroides 2.4.1, Rhodospirillum molischianum and Rhodopseudomonas acidophila. *Chem. Phys. Lett.* **2004**, *390*, 314−322.
(8) Ostroumov, E.; Müller, M. G.; Marian, C. M.; Kleinschmidt, M.; Holzwarth, A. R. Electronic coherence provides a direct proof for energy-level crossing in photoexcited lutein and β-carotene. *Phys. Rev. Lett.* **2009**, *103*, 108302.
(9) Christensson, N.; Milota, F.; Nemeth, A.; Pugliesi, I.; Riedle, E.; Sperling, J.; Pullerits, T.; Kauffmann, H. F.; Hauer, J. Electronic double-quantum coherences and their impact on ultrafast spectroscopy: the example of β-carotene. *J. Phys. Chem. Lett.* **2010**, *1*, 3366−3370.
(10) Marek, M. S.; Buckup, T.; Motzkus, M. Direct observation of a dark state in lycopene using pump-DFWM. *J. Phys. Chem. B* **2011**, *115*, 8328−8337.
(11) Calhoun, T. R.; Davis, J. A.; Graham, M. W.; Fleming, G. R. The separation of overlapping transitions in beta-carotene with broadband 2D electronic spectroscopy. *Chem. Phys. Lett.* **2012**, *523*, 1−5.
(12) Ostroumov, E. E.; Mulvaney, R. M.; Cogdell, R. J.; Scholes, G. D. Broadband 2D electronic spectroscopy reveals a carotenoid dark state in purple bacteria. *Science* **2013**, *340*, 52−56.
(13) Polivka, T.; Sundström, V. Dark excited states of carotenoids: Consensus and controversy. *Chem. Phys. Lett.* **2009**, *477*, 1−11.
(14) Hauer, J.; Maiuri, M.; Viola, D.; Lukes, V.; Henry, S.; Carey, A. M.; Cogdell, R. J.; Cerullo, G.; Polli, D. Explaining the temperature dependence of spirilloxanthin's S* signal by an inhomogeneous ground state model. *J. Phys. Chem. A* **2013**, *117*, 6303−6310.
(15) Enriquez, M. M.; Hananoki, S.; Hasegawa, S.; Kajikawa, T.; Katsumura, S.; Wagner, N. L.; Birge, R. R.; Frank, H. A. Effect of molecular symmetry on the spectra and dynamics of the intramolecular charge transfer (ICT) state of peridinin. *J. Phys. Chem. B* **2012**, *116*, 10748−10756.
(16) Frank, H. A.; Bautista, J. A.; Josue, J.; Pendon, Z.; Hiller, R. G.; Sharples, F. P.; Gosztola, D.; Wasielewski, M. R. Effect of the solvent environment on the spectroscopic properties and dynamics of the lowest excited states of carotenoids. *J. Phys. Chem. B* **2000**, *104*, 4569−4577.
(17) Niedzwiedzki, D. M.; Chatterjee, N.; Enriquez, M. M.; Kajikawa, T.; Hasegawa, S.; Katsumura, S.; Frank, H. A. Spectroscopic investigation of peridinin analogues having different π-electron conjugated chain lengths: Exploring the nature of the intramolecular charge transfer state. *J. Phys. Chem. B* **2009**, *113*, 13604−13612.
(18) Zigmantas, D.; Hiller, R. G.; Sundström, V.; Polivka, T. Carotenoid to chlorophyll energy transfer in the peridinin-chlorophyll-a-protein complex involves an intramolecular charge transfer state. *Proc. Natl. Acad. Sci. U.S.A.* **2002**, *99*, 16760−16765.
(19) Papagiannakis, E.; van Stokkum, I. H. M.; Vengris, M.; Cogdell, R. J.; Van Grondelle, R.; Larsen, D. S. Excited-state dynamics of carotenoids in light-harvesting complexes. 1. Exploring the relationship between the S1 and S* states. *J. Phys. Chem. B* **2006**, *110*, 5727−5736.
(20) Chatterjee, N.; Niedzwiedzki, D. M.; Aoki, K.; Kajikawa, T.; Katsumura, S.; Hashimoto, H.; Frank, H. A. Effect of structural modifications on the spectroscopic properties and dynamics of the excited states of peridinin. *Arch. Biochem. Biophys.* **2009**, *483*, 146−155.
(21) Linden, P. A.; Zimmermann, J.; Brixner, T.; Holt, N. E.; Vaswani, H. M.; Hiller, R. G.; Fleming, G. R. Transient absorption study of peridinin and peridinin-chlorophyll a-protein after two-photon excitation. *J. Phys. Chem. B* **2004**, *108*, 10340−10345.
(22) Shima, S.; Ilagan, R.; Gillespie, N.; Sommer, B.; Hiller, R.; Sharples, F.; Frank, H.; Birge, R. Two-photon and fluorescence spectroscopy and the effect of environment on the photochemical properties of peridinin in solution and in the peridinin-chlorophyll-protein from Amphidinium carterae. *J. Phys. Chem. A* **2003**, *107*, 8052−8066.
(23) Damjanovic, A.; Ritz, T.; Schulten, K. Excitation transfer in the peridinin-chlorophyll-protein of Amphidinium carterae. *Biophys. J.* **2000**, *79*, 1695−1705.
(24) Hsu, C.; Walla, P.; Head-Gordon, M.; Fleming, G. The role of the S-1 state of carotenoids in photosynthetic energy transfer: The light-harvesting complex II of purple bacteria. *J. Phys. Chem. B* **2001**, *105*, 11016−11025.
(25) Vaswani, H.; Hsu, C.; Head-Gordon, M.; Fleming, G. Quantum chemical evidence for an intramolecular charge-transfer state in the carotenoid peridinin of peridinin-chlorophyll-protein. *J. Phys. Chem. B* **2003**, *107*, 7940−7946.
(26) Spezia, R.; Zazza, C.; Palma, A.; Amadei, A.; Aschi, M. A DFT study of the low-lying singlet excited states of the all-trans peridinin in vacuo. *J. Phys. Chem. A* **2004**, *108*, 6763−6770.
(27) Starke, J. H.; Wormit, M.; Schirmer, J.; Dreuw, A. How much double excitation character do the lowest excited states of linear polyenes have? *Chem. Phys.* **2006**, *329*, 39−49.
(28) Dreuw, A.; Wormit, M. Simple replacement of violaxanthin by zeaxanthin in LHC-II does not cause chlorophyll fluorescence quenching. *J. Inorg. Biochem.* **2008**, *102*, 458−465.
(29) Marian, C. M.; Gilka, N. Performance of the DFT/MRCI method on electronic excitation of extended π-systems. *J. Chem. Theory Comput.* **2008**, *4*, 1501−1515.
(30) Kleinschmidt, M.; Marian, C. M.; Waletzke, M.; Grimme, S. Parallel multireference configuration interaction calculations on mini-beta-carotenes and beta-carotene. *J. Chem. Phys.* **2009**, *130*, 044708.
(31) Cerón-Carrasco, J. P.; Requena, A.; Marian, C. M. Theoretical study of the low-lying excited states of β-carotene isomers by a multireference configuration interaction method. *Chem. Phys.* **2010**, *373*, 98−103.
(32) Kusumoto, T.; Horibe, T.; Kajikawa, T.; Hasegawa, S.; Iwashita, T.; Cogdell, R. J.; Birge, R. R.; Frank, H. A.; Katsumura, S.; Hashimoto, H. Stark absorption spectroscopy of peridinin and allene-modified analogues. *Chem. Phys.* **2010**, *373*, 71−79.
(33) Götze, J. P.; Thiel, W. TD-DFT and DFT/MRCI study of electronic excitations in violaxanthin and zeaxanthin. *Chem. Phys.* **2013**, *419*, 247−255.
(34) Schulten, K.; Karplus, M. On the trigin of a tow-tying torbidden transition in tolyenes and telated tolecules. *Chem. Phys. Lett.* **1972**, *14*, 305−309.
(35) Tavan, P.; Schulten, K. The 2 ^1A_g − 1 ^1B_u energy gap in the polyenes: An extended configuration interaction study. *J. Chem. Phys.* **1979**, *70*, 5407−5413.
(36) Premvardhan, L.; Papagiannakis, E.; Hiller, R. G.; Van Grondelle, R. The charge-transfer character of the S0 −> S2 transition in the carotenoid peridinin is revealed by Stark spectroscopy. *J. Phys. Chem. B* **2005**, *109*, 15589−15597.
(37) Grimme, S.; Waletzke, M. A combination of Kohn-Sham density funtional theory and multi-reference configuration interaction methods. *J. Chem. Phys.* **1999**, *111*, 5645−5655.
(38) Silva-Junior, M. R.; Schreiber, M.; Sauer, S. P. A.; Thiel, W. Benchmarks for electronically excited states: Time-dependent density functional theory and density functional theory based multireference configuration interaction. *J. Chem. Phys.* **2008**, *129*, 104103.
(39) Frisch, M. J.; et al. *Gaussian 09*; Gaussian, Inc.: Wallingford, CT, 2009.

(40) *TURBOMOLE V6.3 2011*, a development of University of Karlsruhe and Forschungszentrum Karlsruhe GmbH, 1989−2007, TURBOMOLE GmbH, since 2007; available from: http://www.turbomole.com.
(41) Tomasi, J.; Mennucci, B.; Cammi, R. Quantum mechanical continuum solvation models. *Chem. Rev.* **2005**, *105*, 2999−3094.
(42) Cancès, E.; Mennucci, B.; Tomasi, J. A new integral equation formalism for the polarizable continuum model: theoretical background and applications to isotropic and anisotropic dielectrics. *J. Chem. Phys.* **1997**, *107*, 3032−3041.
(43) Schäfer, A.; Horn, H.; Ahlrichs, R. Fully optimized contracted Gaussian basis sets for atoms Li to Kr. *J. Chem. Phys.* **1992**, *97*, 2571−2577.
(44) Lee, C.; Yang, W.; Parr, R. G. Development of the Colle-Salvetti correlation-energy formula into a functional of the electron density. *Phys. Rev. B* **1988**, *37*, 785−789.
(45) Becke, A. D. A new mixing of Hartree−Fock and local density-functional theories. *J. Chem. Phys.* **1993**, *98*, 1372−1377.
(46) In order to ensure convergence with respect to the initial active space, we carried out a gas-phase single-point calculation at the ground-state CAM-B3LYP structure with an initial MRCI reference space spanned by single and double excitations from the seven highest occupied MOs to the seven lowest unoccupied MOs of the ground state KS determinant. The final excitation energies and properties were identical with the default choice reported in the text within all significant digits.
(47) Marder, S. R.; Gorman, C. B.; Tiemann, B. G.; Perry, J. W.; Bourhill, G.; Mansour, K. Relation between bond-length alternation and second electronic hyperpolarizability of conjugated organic molecules. *Science* **1993**, *261*, 186−189.
(48) Marder, S. R.; Cheng, L.-T.; Tiemann, B. G.; Friedli, A. C.; Blanchard-Desce, M.; Perry, J. W.; Skindhøj, J. Large first hyperpolarizabilities in push-pull polyenes by tuning of the bond length alternation and aromaticity. *Science* **1994**, *263*, 511−514.
(49) Tretiak, S.; Mukamel, S. Density matrix analysis and simulation of electronic excitations in conjugated and aggregated molecules. *Chem. Rev.* **2002**, *102*, 3171−3212.
(50) Hoffmann, M.; Schmidt, K.; Fritz, T.; Hasche, T.; Agranovich, V.; Leo, K. The lowest energy Frenkel and charge-transfer excitons in quasi-one-dimensional structures: application to MePTCDI and PTCDA crystals. *Chem. Phys.* **2000**, *258*, 73−96.
(51) Macernis, M.; Sulskus, J.; Duffy, C. D. P.; Ruban, A. V.; Valkunas, L. Electronic spectra of structurally deformed lutein. *J. Phys. Chem. A* **2012**, *116*, 9843−9853.
(52) Bautista, J.; Connors, R.; Raju, B.; Hiller, R.; Sharples, F.; Gosztola, D.; Wasielewski, M.; Frank, H. Excited state properties of peridinin: observation of a solvent dependence of the lowest excited singlet state lifetime and spectral behavior unique among carotenoids. *J. Phys. Chem. B* **1999**, *103*, 8751−8758.